

1 **Metal binding to the N-terminal cytoplasmic domain of the P_{1B} ATPase HMA4 is**
2 **required for metal transport in *Arabidopsis*.**

3 Clémentine Laurent^{1*}, Gilles Lekeux^{1*}, Ashwinie A. Ukuwela², Zhiguang Xiao², Jean-Benoit
4 Charlier¹, Bernard Bosman³, Monique Carnol³, Patrick Motte^{1,4}, Christian Damblon⁵, Moreno
5 Galleni¹ and Marc Hanikenne^{1,4,\$}

6 ¹ Center for Protein Engineering (CIP), Department of Life Sciences, University of Liège, B-
7 4000 Liège, Belgium

8 ² School of Chemistry and Bio21 Molecular Science and Biotechnology Institute, University
9 of Melbourne, Parkville, Victoria 3010, Australia

10 ³ Laboratory of Plant and Microbial Ecology, Department of Biology, Ecology, Evolution,
11 University of Liège, B-4000 Liège, Belgium

12 ⁴ PhytoSYSTEMS, University of Liège, B-4000 Liège, Belgium

13 ⁵ Chimie Biologique Structurale, Department of Chemistry, University of Liège, Belgium

14 * Equal contributions

15 ^{\$} Corresponding author:

16 Marc Hanikenne

17 email: marc.hanikenne@ulg.ac.be

18 Tel: +32-4-3663844

19 Fax: +32-4-3662960

20 **Acknowledgments**

21 We thank Dr. C. Nouet, S. Fanara, M. Schloesser and M.C. Requier for technical support.
22 Prof. A. Wedd is thanked for his constructive comments and suggestions. We thank Dr. M.
23 Haydon for the kind gift of *hma2hma4* seeds. Funding was provided by the "Fonds de la
24 Recherche Scientifique–FNRS" (FRFC-2.4583.08, PDR-T.0206.13) (MH, MG), the
25 University of Liège (SFRD-12/03) (MH), the Belgian Program on Interuniversity Poles of
26 Attraction (IAP no. P6/19) and the Australian Research Council (grant DP130100728) (AAU,
27 ZX). MH is Research Associate of the FNRS. Doctoral fellowships were funded by the FNRS
28 (CL) and the "Fonds pour la formation à la Recherche dans l'Industrie et dans l'Agriculture"
29 (GL, JBC).

30 **Abstract**

31 P_{IB} ATPases are metal cation pumps that transport metals across membranes. These proteins
32 possess N- and C-terminal cytoplasmic extensions that contain Cys- and His-rich high
33 affinity metal binding domains, which may be involved in metal sensing, metal ion selectivity
34 and/or in regulation of the pump activity. The P_{IB} ATPase HMA4 (Heavy Metal ATPase 4)
35 plays a central role in metal homeostasis in *Arabidopsis thaliana* and has a key function in
36 zinc and cadmium hypertolerance and hyperaccumulation in the extremophile plant species
37 *Arabidopsis halleri*.

38 Here, we examined the function and structure of the N-terminal cytoplasmic metal-binding
39 domain of HMA4. We mutagenized a conserved CCTSE metal-binding motif in the domain
40 and assessed the impact of the mutations on protein function and localization *in planta*, on
41 metal-binding properties *in vitro* and on protein structure by Nuclear Magnetic Resonance
42 spectroscopy.

43 The two Cys residues of the motif are essential for the function, but not for localization, of
44 HMA4 *in planta*, whereas the Glu residue is important but not essential. These residues also
45 determine zinc coordination and affinity. Zinc binding to the N-terminal domain is thus
46 crucial for HMA4 protein function, whereas it is not required to maintain the protein
47 structure.

48 Altogether, combining *in vivo* and *in vitro* approaches in our study provides insights towards
49 the molecular understanding of metal transport and specificity of metal P-type ATPases.

50

51 **Keywords:** metal P-type ATPase, metal binding domain, zinc transport, structure-function
52 analysis, Arabidopsis.

53

54

55 **Introduction**

56 Zinc is an essential transition metal for development and growth of photosynthetic organisms.
57 It plays important roles as enzyme or structural cofactor in many biochemical processes
58 (Broadley et al. 2007; Palmer and Guerinot 2009; Nouet et al. 2011). However, zinc becomes
59 toxic when present in excess in tissues, through unspecific binding or competition with other
60 metals for the active sites in proteins (Goyer 1997; Gaither and Eide 2001; Hall and Williams
61 2003; Tuerk and Fazel 2009). To maintain zinc concentration in tissues within an optimal
62 range, plants have developed a complex and tightly controlled zinc homeostasis network.
63 This network relies in part on zinc membrane transporters that ensure zinc uptake,
64 distribution and storage (Krämer et al. 2007; Palmer and Guerinot 2009; Nouet et al. 2011).

65 In *Arabidopsis thaliana*, *HMA4* (*Heavy Metal ATPase 4*) encodes a zinc and cadmium efflux
66 pump of the IB subfamily of P-type ATPases (or CPx-ATPases) (Williams and Mills 2005;
67 Palmgren and Nissen 2011; Pedersen et al. 2012; Hanikenne and Baurain 2014) and is an
68 essential node of the metal homeostasis network (Mills et al. 2003; Hussain et al. 2004;
69 Verret et al. 2004). Together with its paralog AtHMA2, the HMA4 transporter is localized at
70 the plasma membrane and is expressed in vascular tissues in roots and shoots (Hussain et al.
71 2004; Verret et al. 2004; Siemianowski et al. 2013). AtHMA2 and AtHMA4 are responsible
72 for the translocation of zinc from roots to shoots. A *hma2hma4* double *A. thaliana* mutant
73 displays stunted growth resulting from severe zinc deficiency in shoots (Hussain et al. 2004).
74 AtHMA2 and AtHMA4 are also responsible for cadmium translocation to shoots (Wong and
75 Cobbett 2009; Cun et al. 2014). In addition, the HMA4 protein plays a key role in the zinc
76 and cadmium hyperaccumulation and hypertolerance syndrome in the Brassicaceae
77 *Arabidopsis halleri* (Talke et al. 2006; Courbot et al. 2007; Hanikenne et al. 2008; Hanikenne
78 et al. 2013) and *Noccaea caerulescens* (O' Lochlainn et al. 2011; Craciun et al. 2012), an
79 extreme trait enabling these species to colonize metal-polluted soils (Krämer 2010;
80 Hanikenne and Nouet 2011). In *A. halleri*, high expression of *HMA4* supports high rates of
81 root-to-shoot translocation of zinc mediated by xylem loading (Hanikenne et al. 2008).
82 Increased expression of *HMA4* in *A. halleri* results from tandem triplication and *cis*-
83 activation of expression of all three gene copies that were selected for during the evolutionary
84 history of *A. halleri* (Hanikenne et al. 2008; Hanikenne et al. 2013).

85 P-type ATPases constitute a superfamily of pumps using the energy of ATP to transport
86 cations, and possibly phospholipids (Kühlbrandt 2004; Palmgren and Nissen 2011). P-type

87 ATPases can be divided into five major classes, I–V, based on ion transport specificities and
88 clustering in phylogenetic trees (Axelsen and Palmgren 1998; Palmgren and Nissen 2011).
89 Despite a low sequence conservation, all P-type ATPases share a set of structural and
90 mechanistic features (Toyoshima and Nomura 2002; Toyoshima and Inesi 2004; Toyoshima
91 2008; Toyoshima 2009; Palmgren and Nissen 2011). These proteins are characterized by the
92 phosphorylation of an invariant Asp residue by ATP during the ion transport cycle. During
93 this so-called Post-Albers cycle, the pumps undergo a series of conformational changes upon
94 ion binding/release and phosphorylation/dephosphorylation. These conformational changes
95 allow transport of the ion across the membrane. P-type ATPases possess specific cytoplasmic
96 catalytic domains, the Actuator, Nucleotide and Phosphorylation domains, which are
97 essential for the transport cycle. The transmembrane segments (TM) of P-type ATPases
98 constitute the transport domain, which, determines ion selectivity and thanks to a high
99 flexibility, allows binding and release of the ion (Kühlbrandt 2004; Williams and Mills 2005;
100 Palmgren and Nissen 2011).

101 Proteins of the IB subfamily of P-type ATPases are involved in metal cation transport across
102 membranes (Williams and Mills 2005; Palmgren and Nissen 2011; Pedersen et al. 2012;
103 Hanikenne and Baurain 2014). These proteins possess 8 TMs responsible for metal
104 coordination during transport, notably including a specific metal binding site located in TM6
105 with the conserved Cys-Pro-(Cys/His/Ser) motif and several other conserved residues
106 (Argüello 2003; Pedersen et al. 2012; Hanikenne and Baurain 2014; Wang et al. 2014). Out
107 of 45 P-type ATPases in *A. thaliana*, eight are IB metal ATPases (AtHMA1-8), which can be
108 further divided in subgroups based on metal transport specificity (Axelsen and Palmgren
109 1998; Argüello 2003; Hanikenne et al. 2005; Chan et al. 2010; Pedersen et al. 2012;
110 Hanikenne and Baurain 2014). (i) AtHMA5-AtHMA8 transport monovalent metal cations
111 (e.g. Cu^+) and belong to the ubiquitous IB-1 subclass of metal ATPases found in all domains
112 of life. This subclass includes the two human IB P-type ATPases, ATP7A and ATP7B, which
113 both transport monovalent copper and whose mutations determine Menkes and Wilson
114 diseases, respectively (Lutsenko and Petris 2003). In plants, the PAA1 (AtHMA6) and PAA2
115 (AtHMA8) proteins are responsible for copper transport across the inner envelope and
116 thylakoid membranes, respectively, which is required for copper delivery to plastocyanin
117 (Shikanai et al. 2003; Abdel-Ghany et al. 2005; Bernal et al. 2007). (ii) AtHMA2-4 transport
118 divalent metal cations (e.g. Zn^{2+} and Cd^{2+}) and belong to subclass IB-2 of metal ATPases
119 found in plants and in prokaryotes. (iii) AtHMA1 belongs to subclass IB-4 of metal ATPases

120 and has a broad ion specificity (Ca^{2+} , Cd^{2+} , Zn^{2+} , Cu^{2+}) (Seigneurin-Berny et al. 2006;
121 Moreno et al. 2008; Kim et al. 2009; Boutigny et al. 2014). HMA1 orthologs in plants
122 originate from a horizontal gene transfer from Chlamydiae into the common ancestor of
123 Plantae and all share a non-canonical Ser-Pro-Cys in TM6 (Baum 2013; Hanikenne and
124 Baurain 2014).

125 IB metal ATPases possess N- and C-terminal extensions that contain high affinity metal
126 binding domains (MBDs) rich in Cys and sometimes His residues. For instance, the C-
127 terminal domain of AtHMA4 contains multiple di-Cys motifs and an extended His stretch.
128 This domain may act as a zinc and cadmium sensor regulating the export capacity of the
129 pump and is required for the full function of the protein *in planta* (Baekgaard et al. 2010;
130 Mills et al. 2010).

131 The N-terminal domains of IB-1 copper ATPases are characterized by Cys-x-x-Cys motifs,
132 which are required for copper delivery by metallochaperones, protein activation and/or
133 protein intracellular trafficking. These processes have been described in detail for ATP7A
134 and ATP7B (Barry et al. 2010). In contrast, the N-terminal domain of plant IB-2 zinc
135 ATPases possess a Cys-Cys-x-x-Glu conserved metal-binding motif (CCxxE) within a
136 $\beta\alpha\beta\beta\alpha\beta$ ferredoxin fold. This non-canonical site binds one zinc atom (Eren et al. 2007;
137 Zimmermann et al. 2009). Deletion of the AtHMA2 N-terminal domain results in decreased
138 ATPase activity (Eren et al. 2007) and in failure to complement the phenotype of the
139 *hma2hma4 A. thaliana* mutant (Wong et al. 2009). Mutation of the two Cys residues of the
140 motif into Ala equally impairs the function of the protein *in vivo* (Wong et al. 2009). The N-
141 terminal domain of AtHMA2 is thus essential for function *in planta*. Finally, the N-terminal
142 domain of AtHMA4 was characterized using Nuclear Magnetic Resonance (NMR) and metal
143 probes, which revealed zinc binding by the Cys and Glu residues of the $\text{C}^{27}\text{CTSE}^{31}$ motif and
144 showed that its affinity for zinc was in the subnanomolar range (Zimmermann et al. 2009).
145 The two Cys residues of the motif were required for function of AtHMA4 in yeast (Verret et
146 al. 2005).

147 Conserved MBD motifs in the N-terminal domain of copper IB P-type ATPases have distinct
148 functions in different proteins or even different functions when present in tandem in the same
149 protein ((Tsivkovskii et al. 2001; Mana-Capelli et al. 2003; Mandal et al. 2003; Argüello et
150 al. 2007; Veldhuis et al. 2009; Palmgren and Nissen 2011; Drees et al. 2015). It is thus
151 important to examine differences and commonalities in the role of the N-terminal domains

152 and their conserved MBDs for several IB P-type ATPases. Moreover, many examples exists
153 in the literature illustrating the fact that the functional analysis of IB P-type ATPase MBDs
154 may result in differing observations between *in vivo* and *in vitro* experiments, and also
155 depending on the experimental setup (see for instance, Eren et al. 2007; Wong et al. 2009;
156 Baekgaard et al. 2010; Mills et al. 2010; Drees et al. 2015). Here, to further advance our
157 understanding of structure/function relationship in the HMA4 N-terminal domain, a range of
158 mutants of the C²⁷CTSE³¹ conserved motif were characterized by complementary *in vivo* and
159 *in vitro* approaches. Our data highlight the key function of the domain *in planta* and reveal
160 predominance of the two Cys residues for zinc coordination and affinity.

161

162

163 **Materials and methods**

164 **Plant material, transformation and growth conditions**

165 *A. thaliana* L. Heynhold (accession Columbia, Col-0) and the *A. thaliana hma2hma4* double
166 mutant (Hussain et al. 2004) were used in all experiments. For genetic transformation of the
167 *hma2hma4* mutant, plants were cultivated on soil watered with a 1mM ZnSO₄ solution in a
168 controlled climate room at 22°C and a 8h day⁻¹ photoperiod (short days) during 8 weeks.
169 Plants were then transferred in a 16h day⁻¹ photoperiod (long days) growth chamber to induce
170 flowering and were watered with 3mM ZnSO₄ for 5 weeks. The *hma2hma4* plants were then
171 transformed using *Agrobacterium tumefaciens* by floral dipping (Clough and Bent 1998).
172 GFP fusions were transformed into Col-0 wild-type plants.

173 For experiments, homozygous transgenic seeds (T3 generation) were germinated on 1/2 MS
174 agar medium containing 1% sucrose in short days, after a 5 day incubation at 4°C. After 18
175 days, seedlings were transferred on soil for phenotyping or into hydroponic trays (Araonics,
176 Tocquin et al. 2003) containing modified Hoagland solution as described (Talke et al. 2006;
177 Charlier et al. 2015; Nouet et al. 2015). For soil experiments, plants were watered with
178 distilled water and grown for 2 weeks in short days followed by 5 weeks in long days. For
179 hydroponic experiments, plants were grown for 2 weeks in control conditions (1 μM ZnSO₄)
180 in short days. Plants were then transferred in long days to initiate the treatments: 0.05μM
181 CdSO₄ or 0.2μM ZnSO₄ (Nouet et al. 2015). Nutrient solutions were changed weekly during

182 4 weeks. Root and shoot samples were then harvested separately before processing for ICP-
183 AES analyses.

184 **Cloning**

185 To construct the *pAtHMA4-AhHMA4* cassette and the C²⁷CTSE³¹ variants, the *AtHMA4*
186 promoter (*pAtHMA4*, 2595 bp, Hanikenne et al. 2008) was amplified from Col-0 genomic
187 DNA by PCR using primers harbouring 5'-*AscI* and 3'-*AcyI* restriction sites (Table S1A),
188 respectively. The promoter fragment was cloned into the *AscI* and *AcyI* sites of a *pAhHMA4-*
189 *l-AhHMA4* pBluescript II KS+ vector (Hanikenne et al. 2008) in replacement of *pAhHMA4-*
190 *l*. This vector served as a template for the site-directed mutagenesis of the conserved N-
191 terminal C²⁷CTSE³¹ motif as described (Talke et al. 2006) using mutagenic primers (Table
192 S1B). The wild-type and variant versions of *pAtHMA4-AhHMA4* were then excised by
193 digestion with *AscI* and *PacI* and cloned at the corresponding sites of a promoter-less variant
194 of the pMDC32 vector (Curtis and Grossniklaus 2003; Hanikenne et al. 2008).

195 For localization experiments, the wild-type and variant versions of *AhHMA4* were cloned at
196 the *PacI* and *AscI* sites (Table S1A) in fusion with GFP into the pMDC83 vector allowing
197 expression under the control of a double 35S promoter (Curtis and Grossniklaus 2003).

198 For production in *E. coli*, a synthetic gene encoding the N-terminal part of the *A. halleri*
199 HMA4 protein (AhHMA4n, residues 1-95) with optimized codon usage was obtained from
200 GeneArt. The fragment was subsequently cloned into the pET9a expression vector (Novagen)
201 using *NdeI* and *BamHI* restriction sites. Variants with mutations in the C²⁷CTSE³¹ motif were
202 obtained as above using the pET9a-AhHMA4n vector as template (see mutagenic primers in
203 Table S1B).

204 All final constructions were verified by sequencing.

205 **RNA Extraction, cDNA Synthesis, and Quantitative RT-PCR**

206 Total RNAs were prepared using the RNeasy Plant Mini kit with on column DNase
207 treatment (Qiagen), and cDNAs were synthesized using the RevertAid H Minus First Strand
208 cDNA Synthesis kit with Oligo dT (Thermo Scientific). Transcript levels were determined by
209 real-time RT-PCR in 384-well plates with an ABI Prism 7900HT system (Applied
210 Biosystems) using MESA GREEN qPCR MasterMix (Eurogentec) as described (Talke et al.,
211 2006; Nouet et al. 2015) including 4 technical replicates for each sample/primer pair (Online

212 Resource 2). The quality of the PCRs was checked visually through analysis of dissociation
213 and amplification curves. Relative gene expression levels were determined by normalization
214 using multiple reference genes with the qBase software (Biogazelle, Hellemans et al. 2007).
215 Three reference genes (*At1g18050*, *UBQ10*, *EFL1a*) were selected from the literature
216 (Czechowski et al. 2005). Their adequacy to normalize gene expression in our experimental
217 conditions was verified using the geNorm software in qBase (gene stability measure
218 $M=0.404$, pairwise variation $CV=0.155$) (Vandesompele et al. 2002).

219 **ICP-AES analyses**

220 For plant samples, shoot tissues were rinsed in milliQ water, whereas root tissues were
221 desorbed and washed as described (Talke et al. 2006). Tissues were then dried at 60°C for 2
222 days. For protein samples, proteins were dialyzed against the purification buffer A without
223 zinc (see below). Samples (10-50 mg of tissues, 5-10 μ M purified proteins) were then acid-
224 digested in DigiPrep tubes with 3 ml $\geq 65\%$ (w/w) HNO_3 (Sigma-Aldrich) on a DigiPrep
225 Graphite Block Digestion System (SCP Science) as follows: 15 min at 45°C, 15 min at 65°C
226 and 90 min at 105°C. After cooling, sample volumes were adjusted to 10 ml with milliQ
227 water and 200 μ l $\geq 65\%$ HNO_3 (Sigma-Aldrich). Metal concentrations were determined by
228 ICP-AES (Inductively Coupled Plasma-Atomic Emission Spectroscopy, Vista AX, Varian).

229 **GFP imaging**

230 Leaves of eighteen day-old T1 seedlings expressing the GFP fusions described above were
231 analyzed (3 independent lines per construct). Images were collected using a SP2 inverted
232 confocal microscope (Leica). An Argon/Ion laser (488nm) was used for excitation of the GFP
233 protein and the emission light was dispersed and recorded at 500 to 540 nm, as described
234 (Rausin et al. 2010). To induce plasmolysis, seedlings were incubated in a 6% (w/v) NaCl
235 solution for 5 minutes prior observation.

236

237 **Production and purification of non-labelled and isotope-labelled N-terminal domains**

238 *E. coli* cells (strain BL21 (DE3)) transformed with the pET9a/AhHMA4n expression vector
239 were grown at 37°C in 2 L of LB (Luria-Bertani) medium containing 50 μ M ZnCl_2 and
240 50 μ g/mL kanamycin. At an OD_{600} of ~ 0.8 , the production was directly induced with 1mM
241 IPTG (isopropyl β -D-thiogalactopyranoside). The culture was then incubated for 18h at 18°C.

242 The cells, collected by centrifugation, were resuspended in 50 mL of 10 mM Tris/HCl pH 8
243 supplemented by 1 mM TCEP and 50 μ M ZnCl₂ (buffer A). A protease inhibitor cocktail
244 (mini complete EDTA-free, Roche) was added to avoid the degradation of the protein.

245 For isotope labelling, prior induction of expression, cells were harvested an OD₆₀₀ of ~0.8 by
246 centrifugation at 11000g for 20 min and resuspended in 500 ml of M9 medium containing
247 [¹⁵N]NH₄Cl and/or [¹³C]Glucose (Cambridge Isotope Laboratories, Inc.), 50 μ M ZnCl₂ and
248 50 μ g/mL kanamycin. After 1h incubation at 37°C, the expression of the protein was induced
249 by 1mM IPTG. Labelled proteins were then collected as described above.

250 In all cases, cells were lysed after harvest using an EmulsiFlex-C3 cell disrupter (Avestin).
251 The cellular extracts were clarified by centrifugation at 48000g for 40 min at 4°C. The
252 soluble fraction was then loaded onto a cation exchange sepharose column (24 mL, GE
253 Healthcare) equilibrated in 10mM Tris/HCl pH 8 supplemented with 1mM TCEP and 50 μ M
254 ZnCl₂. The bound proteins were eluted over a 250 mL linear NaCl gradient (0-300mM). The
255 fractions containing AhHMA4n were pooled, dialyzed overnight against buffer A (see above)
256 and then further purified on a 5 mL Poros HS column (Applied Biosystems). The proteins
257 were eluted thanks to a linear NaCl gradient as above.

258 The N-terminal domain variants were purified as described for the native AhHMA4 N-
259 terminal domain. However, for variants C²⁷A, C²⁸A and C²⁷A/C²⁸A/E³¹A, purification
260 conditions were slightly different: (i) 10mM Tris/HCl pH 8, 1mM TCEP, 50 μ M ZnCl₂ and
261 0.02% n-Dodecyl β -D-Maltopyranoside was used for equilibration and (ii) the elution
262 gradient was increased to 1 M NaCl.

263 The AhHMA4n fractions were concentrated by ultrafiltration on a 3 kDa molecular-mass cut-
264 off column (Vivaspin). The protein purity was assessed by SDS/PAGE (18% gels), and the
265 final protein concentration was determined by using the molar absorption coefficient at 280
266 nm ($\epsilon=8480 \text{ M}^{-1}\text{cm}^{-1}$), which was calculated with the help of ProtParam (ExpPASy
267 Proteomics Server, <http://expasy.org/>).

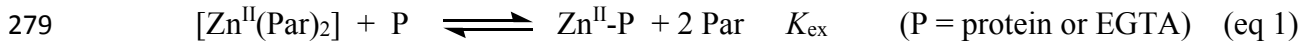
268 **Determination of the affinity of HMA4n for zinc**

269 The AtHMA4n control was produced as reported previously (Zimmermann et al. 2009). The
270 oxidised AhHMA4n protein with an internal disulphide bond (i.e. AhHMA4n-SS) was
271 produced by quantitative oxidation of AhHMA4n with stoichiometric amount of

272 $[\text{Fe}^{\text{III}}(\text{CN})_6]^{3+}$ and purified by an ion-exchange column. The AhHMA4n native and variant
 273 proteins were produced as described above. To ensure a complete removal of all metal ions
 274 from the samples, they were incubated with excess EDTA, followed by a gel-filtration
 275 separation.

276 The determination of zinc (Zn^{II}) affinity was conducted via the competition reaction 1 and the
 277 data analysed via equation 2 (Xiao et al. 2013):

278



280

281

282

283
$$\frac{[\text{P}]_{\text{tot}}}{[\text{Zn}]_{\text{tot}}} = K_{\text{D}} \beta_2 \left(\frac{[\text{Par}]_{\text{tot}}}{[\text{Zn}^{\text{II}}(\text{Par})_2]} - 2 \right)^2 [\text{Zn}^{\text{II}}(\text{Par})_2] \left(1 - \frac{[\text{Zn}^{\text{II}}(\text{Par})_2]}{[\text{Zn}]_{\text{tot}}} \right) + 1 - \frac{[\text{Zn}^{\text{II}}(\text{Par})_2]}{[\text{Zn}]_{\text{tot}}} \quad (\text{eq 2})$$

284

285

286 The term $[\text{Zn}^{\text{II}}(\text{Par})_2]$ is the equilibrium concentration of probe complex $[\text{Zn}^{\text{II}}(\text{Par})_2]$ in eq 1
 287 and may be determined directly from the solution absorbance at 500 nm after subtracting the
 288 minor contribution from the Par ligand. The other terms in eq 2 are the known total
 289 concentrations of the relevant species. The term $K_{\text{D}} \beta_2 = (K_{\text{ex}})^{-1}$ is a constant under fixed
 290 conditions and may be derived by curve-fitting of the experimental data to eq 2. However, the
 291 accumulated formation constant β_2 for $\text{Zn}^{\text{II}}(\text{Par})_2$ varies considerably with experimental
 292 conditions and this will affect the reliability of K_{D} for $\text{Zn}^{\text{II}}\text{-P}$ (Zimmermann et al. 2009). To
 293 control such variation, the EGTA ligand, whose affinities for Zn^{II} at various pH values are
 294 known, was used as a control affinity calibrator under each experimental condition.
 295 Consequently, the K_{D} for $\text{Zn}^{\text{II}}\text{-P}$ may be obtained reliably via eq 3 relative to a control
 296 experiment in the same reaction medium with $\text{P} = \text{EGTA}$ in eq 1:

297
$$K_{\text{D}}(\text{Zn}^{\text{II}}\text{-P}) = [K_{\text{ex}}(\text{EGTA}) / K_{\text{ex}}(\text{P})] \times K_{\text{D}}(\text{Zn}^{\text{II}}\text{-EGTA}) \quad (\text{eq 3})$$

298 The experiments were conducted in MOPS buffer (50 mM, pH 7.3, 100 mM NaCl) with the
 299 detailed procedure following that reported previously (Zimmermann et al. 2009). To ensure a
 300 complete reduction of all protein thiols, reductant TCEP (100 μM) was included in all
 301 reaction media (except for the experiments with the oxidised HMA4n sample). Control
 302 experiments showed that excess TCEP had no discernible impact on the estimated $\text{Zn}(\text{II})$
 303 affinity.

304 Nuclear Magnetic Resonance analysis

305 The spectral assignment experiment of the native and C²⁷A/C²⁸A/E³¹A triple mutant HMA4n
306 domains were performed on 0.5 mM ¹³C- and ¹⁵N-labelled samples while the HSQC
307 experiments on the single mutants (C²⁷A, C²⁸A and E³¹A) were conducted on 0.07-0.14 mM
308 ¹⁵N-labelled samples. The apo form of AhHMA4n was obtained by treating 100μM of
309 protein with 400μM EDTA for 10 minutes. All samples were prepared in a buffer containing
310 10mM NH₄Ac, 1mM TCEP, 100mM NaCl at pH 6.6 with 5% D₂O and DSS 10 μM. The
311 different spectra were acquired at 293 K on a Bruker AVI 500MHz spectrometer equipped
312 with a TCI cryogenically cooled probe. The spectra of the 2D (¹H-¹⁵N HSQC) and 3D
313 [HNCA, HNCOC, HNCACB and CBCA(CO)NH] (Cavanagh 1996) experiments were
314 processed using TOPSPIN (Bruker) and analyzed with CCPNmr.

315 **NMR Minimum Chemical Shift Perturbation**

316 The effects of N-terminal domain mutations on the amide NH resonances were analysed as
317 follows. For each cross-peak in the 1H-15N HSQC spectrum of the wild-type protein, the
318 nearest cross-peak (in terms of 1H and 15N chemical shifts) in the spectrum of each mutant
319 was identified. The 1H and 15N chemical shift differences, ΔH and ΔN, between each such
320 pair of cross-peaks were measured and used to calculate a “minimum Chemical Shift
321 Perturbation” (mCSP) (Lian et al. 2000).

$$322 \quad mCSP = \sqrt{(6.7\Delta H)^2 + \Delta N^2}$$

323 While the individual chemical shifts may be underestimated, the perturbed amide NH can be
324 reliably identified (Williamson et al. 1997). The minimum chemical shift is plotted as a
325 function of residue number. The calculations were performed using TOPSPIN (*xpk) peak
326 lists and a custom made tcl script.

327 A threshold value was estimated in order to determine significant CSP. In a first step, all CSP
328 are considered and the average (<CSP>) plus three times the standard deviation (σ) is
329 calculated. Then, the highest CSP (CSP ≥ <CSP> + 3σ) are removed from the data and new
330 average and new standard deviation are calculated. The operation is repeated until
331 convergence is reached. The final value <CSP> + 3σ for the residues not significantly
332 perturbed corresponds to the threshold (Tavel et al. 2012).

333 **Statistical analysis**

334 All statistical analyses of the data were carried out using STATISTICA (Statsoft).

335

336 **Results**

337 In this study, we selected the *A. halleri* HMA4 protein as an experimental system to examine
338 *in vivo* and *in vitro* the function of the conserved N-terminal C²⁷CTSE³¹ metal binding motif.
339 The AtHMA4 and AhHMA4 protein share 96.8% identity over the 95 residue N-terminal
340 domain (Online Resource 1).

341 **The C²⁷CTSE³¹ motif of the N-terminal domain is essential for the function of the** 342 **HMA4 protein *in vivo***

343 To examine *in vivo* the function of the C²⁷CTSE³¹ N-terminal motif of HMA4 (Zimmermann
344 et al. 2009), we separately mutated the two Cys and the Glu residues into Ala. A triple
345 mutant, where the two Cys and the Glu were mutated into Ala, was also generated (Fig. 1a).
346 The native (*AhHMA4*) and mutated genes were expressed under the control of the
347 endogenous *A. thaliana* HMA4 promoter (pAtHMA4) in the loss-of-function *hma2hma4* *A.*
348 *thaliana* mutant (Hussain et al. 2004). Several independent homozygous transgenic lines (T3
349 generation) were obtained for each construct. The HMA4 gene variants were expressed at
350 similar levels in plant tissues (Online Resource 2).

351 In our growth conditions on standard soil watered with tap water, the expression of *AhHMA4*
352 rescued the phenotype of the *hma2hma4* mutant. The plants developed normally and were
353 able to flower and set seeds without additional zinc supply in the soil, as Col-0 wild-type
354 plants (Fig. 1b-e). In contrast, expression of the C²⁷CTSE³¹ motif variants resulted in the
355 absence of (C²⁷A, C²⁸A, triple mutant) or in partial (E³¹A) complementation, respectively
356 (Fig. 1f-j). Indeed, plant expressing the C²⁷A, C²⁸A and triple mutants displayed the stunted
357 growth and chlorotic phenotype typical of the *hma2hma4* mutant (Hussain et al. 2004; Wong
358 and Cobbett 2009; Mills et al. 2010). These plants could complete their life cycle and set
359 seeds only upon massive external zinc supply. The plants expressing the E³¹A mutant
360 presented a phenotype intermediate between Col-0 and *hma2hma4* plants, with a larger
361 rosette and the development of flowers (Fig. 1f). The plants however required additional zinc
362 supply to complete their life cycle. Note that similar results were obtained upon expression of
363 the variants under the control of the *A. halleri* HMA4-1 promoter (data not shown, Hanikenne
364 et al. 2008).

365 **Mutations in the C²⁷CTSE³¹ motif alter zinc and cadmium distribution in plant tissues**

366 We next determined if the mutation in the C²⁷CTSE³¹ motif altered metal accumulation in
367 plant tissues. Zinc and cadmium concentrations were measured by ICP-AES in roots and
368 rosette leaves of 8 week old wild-type (Col-0) and *hma2hma4* plants as well as transgenic
369 plants expressing the C²⁷CTSE³¹ variants after cultivation for four weeks in Hoagland
370 hydroponic medium containing either 0.2 μM Zn or 0.05 μM Cd (Nouet et al. 2015). The
371 *hma2hma4* mutant accumulated about 6-fold higher zinc and 4-fold higher cadmium in roots
372 and 2.2-fold lower zinc and 6-fold lower cadmium in shoots than the wild-type, respectively
373 (Fig. 2). This reflected the inability of the *hma2hma4* mutant to translocate zinc and cadmium
374 from root to shoot. Expression of the native *AhHMA4* gene in the *hma2hma4* genetic
375 background almost completely restored wild-type levels of zinc accumulation in root and
376 shoot tissues. The plants expressing the C²⁷A, C²⁸A and triple mutants accumulated zinc at
377 levels identical to the *hma2hma4* mutant. In contrast, expression of the E³¹A mutant partially
378 restored shoot zinc accumulation to levels intermediate between Col-0 and the *hma2hma4*
379 mutant, but only marginally reduced root accumulation (Fig. 2a-b). Identical observations
380 were made upon 0.05 μM Cd exposure (in the presence of 1 μM Zn): only the expression of
381 the E³¹A mutant resulted in moderate increase of cadmium accumulation in shoots compared
382 to the *hma2hma4* mutant (Fig. 2c-d).

383 **The C²⁷CTSE³¹ motif is not required for plasma membrane localization**

384 Mutations in the N-terminal domain of AhHMA4 might impact its intracellular localization.
385 The inability of the C²⁷CTSE³¹ motif variants to complement the phenotype of the *hma2hma4*
386 mutant may therefore results from a mis-localization of the protein in cells rather than a loss
387 of function. To exclude this hypothesis and to ascertain that the variants are expressed at the
388 protein level, we expressed GFP fusions of the C²⁷CTSE³¹ AhHMA4 variants under the
389 control of a double 35S promoter in the Col-0 genetic background.

390 Leaves of 18-day-old seedlings expressing the GFP fusions were imaged by confocal
391 microscopy. All three simple mutants (C²⁷A, C²⁸A and E³¹A) and the triple mutant of the
392 AhHMA4 protein were expressed and localized in the plasma membrane of leaf epidermal
393 cells (Fig. 3). The induction of a plasmolysis of leaf cells confirmed the plasma membrane
394 localization of the protein: a characteristic detachment of the membrane from the cell-wall,
395 with the exception of plasmodesmata, was observed (Fig. 3f). No fluorescence was detected
396 in leaves of Col-0 seedlings using identical settings (Fig. 3a). GFP imaging experiments also

397 suggests that the C²⁷CTSE³¹ motif variant proteins are stable *in planta*, as we did not detect
398 any GFP aggregation in cells (Fig. 3).

399 **Mutations in the C²⁷CTSE³¹ motif alter zinc binding properties *in vitro***

400 The native N-terminal domain of AhHMA4 (residues 1-95 residues, AhHMA4n) and the
401 C²⁷CTSE³¹ variants were expressed in *E. coli* and purified. After dialysis, we assessed the
402 stoichiometry of zinc binding to the proteins by ICP-AES measurements (Table 1). The
403 native AhHMA4n bound ~1 zinc ion per protein. Zinc binding was strongly reduced for the
404 C²⁷A and C²⁸A mutant proteins as well as for the triple mutant. The E³¹A mutant retained an
405 intermediate zinc binding capacity (Table 1).

406 Using the Par zinc probe (Zimmermann et al. 2009), we next quantitatively estimated the
407 binding affinity of the AhHMA4n variants for zinc (Table 2 and Online Resource 3). The
408 native AhHMA4n protein had a K_D for zinc in the nanomolar range identical to that for the
409 AtHMA4n protein (previously determined by Zimmermann et al. 2009), despite 3
410 polymorphic positions in the N-terminal domain (see Online Resource 1). Oxidation of the
411 two Cys thiols to an internal disulfide bond in the binding motif completely abolished zinc
412 binding. The C²⁷A mutation, taken as a representative of the most affected mutant variants,
413 decreased affinity for zinc by 1.8 orders of magnitude, whereas the E³¹A mutation only
414 reduced the affinity for zinc by 1.4 orders of magnitude.

415 **Structural impact of the C²⁷CTSE³¹ motif mutations by NMR spectroscopy**

416 To examine the structural consequences of mutations in the C²⁷CTSE³¹ motif of AhHMA4,
417 2D 15N-1H HSQC NMR experiments were recorded for the native and C²⁷CTSE³¹ variant
418 AhHMA4n proteins. Backbone NH NMR signal chemical shifts and intensities are very
419 sensitive probes to study protein structural and dynamic modifications. The HSQC spectrum
420 of the native AhHMA4n protein was similar to previously published data for AtHMA4n
421 (Zimmermann et al. 2009). The HSQC spectra of the C²⁷CTSE³¹ motif variants revealed that
422 the AhHMA4n domains were structured, despite (strongly) reduced zinc binding capability
423 (Table 1), and displayed limited variations compared to the spectrum of the native
424 AhHMA4n domain (Fig. 4 and Online Resource 4). These observations suggested that
425 mutations in the C²⁷CTSE³¹ motif had limited impact on the domain structure. To statistically
426 support these conclusions, an analysis of the minimal chemical shift perturbations (mCSP)
427 was used to compare the HSQC spectra of the native and C²⁷CTSE³¹ variant AhHMA4n

428 proteins (Fig. 5a and Online Resource 5). The observed mCSPs corresponded to the mutated
429 amino acid residues and to amino acid residues interacting with the mutated residues (Fig. 5).
430 A very similar mCSP profile was also obtained for the apo form of the protein obtained by
431 treatment with EDTA prior to NMR analysis (Online Resource 6).

432 Backbone assignment (N, H, CO, Ca, Cb) was performed for the native AhHMA4n protein
433 and the triple C²⁷A/C²⁸A/E³¹A mutant, which represented the most extreme modification of
434 the C²⁷CTSE³¹ motif. This confirmed that perturbed amino acid residues are located at the
435 vicinity of the zinc binding site or correspond to more distant residues in the primary
436 sequence that are spatially close in the 3D structure. Structure predictions using the backbone
437 chemical shift and the Talos⁺ software (Shen et al. 2009) confirmed that the mutations in the
438 C²⁷CTSE³¹ motif did not have a major impact on the AhHMA4n domain secondary structure
439 (data not shown).

440 **Discussion**

441 IB P-type ATPase proteins play essential roles in metal homeostasis in *Arabidopsis* species
442 (Williams and Mills 2005; Nouet et al. 2011). Hence, HMA4 is a major actor in Zn
443 hyperaccumulation as well as Zn and Cd tolerance in *Arabidopsis halleri* (Talke et al. 2006;
444 Courbot et al. 2007; Willems et al. 2007; Hanikenne et al. 2008; Hanikenne et al. 2013). If
445 the catalytic mechanism of transport by P-type ATPases is well described, establishing the
446 roles and functions of N- and C-terminal extremities and their MBDs still require further
447 investigations. Depending on the organisms and proteins, N-terminal MBDs have been
448 involved in multiple functions, including regulatory roles, controlling catalytic activities,
449 dephosphorylation and metal ion release possibly via interactions with the cytoplasmic ATP
450 binding domain, or the intracellular targeting of the protein (Tsivkovskii et al. 2001; Mana-
451 Capelli et al. 2003; Mandal et al. 2003; Argüello et al. 2007; Veldhuis et al. 2009).

452 Zimmermann et al. (2009) determined the 3D solution structure of the N-terminal domain of
453 AtHMA4, which binds one zinc atom at the C²⁷CTSE³¹ motif. Here, we examined the
454 function of this motif *in planta*, assessed the contribution of the conserved Cys and Glu
455 residues to zinc binding and evaluated the impact of mutations in the motif on protein
456 structure and function. Combining both *in vivo* and *in vitro* analyses allowed an integrated
457 analysis of the structure/function relationship for the N-terminal MBD of HMA4.

458 The HMA4 protein localizes to the plasma membrane in plant tissues (Verret et al. 2004;
459 Courbot et al. 2007; Siemianowski et al. 2013; Nouet et al. 2015). The N-terminal domain of
460 HMA4 was not involved in protein intracellular localization or in protein stability (Fig. 3).
461 Indeed, all mutant variants in fusion with GFP localized in the plasma membrane of stable *A.*
462 *thaliana* transformants (Fig. 3), in agreement with previous results for AtHMA2 (Wong et al.
463 2009). In contrast, the C-terminal domain of AtHMA2 possibly contains a signal important
464 for the subcellular localization of the protein *in planta* (Wong et al. 2009), whereas the C-
465 terminal domain of AtHMA4 is not required for correct localization in yeast cells (Baekgaard
466 et al. 2010).

467 Expression of the *AhHMA4* gene under the control of the pAtHMA4 promoter only partially
468 complemented the defect in root to shoot zinc translocation of the *hma2hma4* mutant: zinc
469 shoot accumulation level was lower than in the wild-type, but was however sufficient to
470 sustain normal development (Figs. 1 and 2). When expressed under the control in the *HMA4*
471 endogenous promoter, *HMA4* is thus not sufficient alone to fully compensate for the loss of
472 both *HMA2* and *HMA4*. In contrast, expressing the same gene under the control of promoters
473 of the *A. halleri HMA4*, which are stronger than the pAtHMA4 promoter (Hanikenne et al.
474 2008) fully complemented the mutant (Nouet et al. 2015).

475 In complementation experiments, the C²⁷A, C²⁸A and C²⁷A/C²⁸A/E³¹A mutations abolished
476 the ability of the AhHMA4 protein to complement the strong zinc deficiency phenotype and
477 to restore zinc and cadmium root-to-shoot translocation in the *hma2hma4 A. thaliana* mutant
478 (Fig. 1 and 2). Reduced zinc binding and affinity (Tables 1 and 2, Online Resource 3) are
479 thus accompanied by a loss of function *in planta*. Previous studies analysing the N-terminal
480 MDB of AtHMA2 (~ 82% sequence identity with the AtHMA4 N-terminal domain, see
481 Online Resource 1) suggested that the CCxxE motif is required for zinc and cadmium binding
482 *in vitro* and for maximum enzyme turnover but were not essential for activity or metal
483 binding to transmembrane metal binding sites in yeast cells (Eren et al. 2007). However, the
484 two Cys residues of the motif were required for function of AtHMA2 *in planta* (Wong et al.
485 2009) and AtHMA4 in yeast (Verret et al. 2005).

486 In contrast, the E³¹A mutation sustained partial complementation of the *hma2hma4* mutant
487 phenotype (Fig. 1 and 2) and retained higher zinc binding and affinity than the Cys-->Ala
488 mutants (Tables 1 and 2, Online Resource 3). Note that this mutant retained a higher capacity
489 for zinc translocation to the shoot than for cadmium (Fig. 2).

490 The NMR HSQC spectrum of the amide NHs of the purified AhHMA4n protein was nearly
491 identical to the data obtained by Zimmermann et al. for AtHMA4n (Zimmermann et al.
492 2009). Since NMR chemical shifts are very sensitive to the structural environment, the very
493 similar NMR spectrum was a strong evidence for a very similar 3D structure. This confirmed
494 the global ferredoxin $\beta\alpha\beta\beta\alpha\beta$ fold of the domain, in which the thiols of Cys residues and
495 carboxy group of the Glu residue contributed to the coordination of zinc. The three
496 polymorphic residues between AtHMA4n and AhHMA4n had thus no major impact on
497 protein structure. Furthermore, we showed here that the mutations in the C²⁷CTSE³¹ motif of
498 AhHMA4n, which drastically reduced zinc binding, had no significant effect either on the
499 secondary or on the tertiary structure of the protein. This observation was also confirmed by
500 the structural analysis of the apo form of AhHMA4n: the structure of the apo form is not
501 altered.

502 Altogether, our data indicated that the two Cys residues of the C²⁷CTSE³¹ motif of the N-
503 terminal MBD are essential for the function of HMA4, whereas the Glu residue is important
504 but not essential. Moreover, zinc binding to the N-terminal MBD is crucial for HMA4 protein
505 function, whereas it is not required to maintain the N-terminal domain structure. Based on
506 these observations arises the following question: what is the requirement of zinc binding for
507 the protein function? It may be required for intramolecular interactions controlling the
508 pump's activity and/or conformational changes during metal transport (Tsivkovskii et al.
509 2001).

510 Copper IB pType ATPases and many bacterial zinc IB pType ATPases possess a highly
511 conserved CxxC motif in their N-terminal MDBs. This motif can bind both monovalent (Cu⁺)
512 or divalent (Cu²⁺, Zn²⁺, Cd²⁺) metal ions *in vitro* and, for instance, metal selectivity for Cu⁺ is
513 determined *in vivo* by electrostatic and hydrophobic interactions with specific copper
514 chaperones (Argüello et al. 2007). However, in all plant zinc IB pType ATPases, this
515 conserved motif is replaced by a CCxxE motif. It was initially suggested that the CCxxE
516 motif could confer selectivity for Zn(II) but not for Cu(I) due to its higher binding affinity for
517 Zn(II) than for Cu(I) (Eren et al. 2007). However, this conclusion has been questioned when
518 both CCxxE and CxxC motifs were showed to bind Cu(I) with affinities at least 6 orders of
519 magnitude higher than Zn(II). Both motifs can also bind Zn(II) with moderate affinities in the
520 nanomolar range (Zimmermann et al. 2009). Quantitative evaluations under identical
521 conditions revealed that the MBDs containing the CCxxE motif bind Zn(II) with affinities
522 20-30 times stronger than do those MBDs containing CxxC while relative affinities for Cu(I)

523 are inverted by a factor of 30-50 (Zimmermann et al. 2009). Consequently, it was proposed
524 that, under metal-limiting conditions, zinc selectivity is conferred by relative affinities and
525 not absolute affinities. Under these conditions, Cu(I) ions are confined to their native high
526 affinity sites and are not available to compete for native Zn(II) sites (Zimmermann et al.
527 2009). Interestingly, the affinity for zinc of the E³¹A domain of HMA4 featuring a CCxxA
528 metal binding motif is essentially identical to that of the N-terminal domain of the copper
529 ATPase HMA7 containing a CxxC metal binding motif (Zimmermann et al. 2009). Yet, in
530 the *hma2hma4 A. thaliana* mutant, the endogenous copper ATPases, such as HMA5 (Andrés-
531 Colás et al. 2006; Kobayashi et al. 2008) or HMA7, do not seem to substitute HMA2 and
532 HMA4 for Zn/Cd transport while the AhHMA4 E³¹A variant did partially sustain the Zn/Cd
533 transport function. It appears that the functional specificity of different metal transporters
534 must also depend on factors other than the metal-binding affinity and that these may include
535 specific intra-molecular interactions (Tsivkovskii et al. 2001) or expression patterns.
536 Interestingly, bacterial zinc (ZntA) and cadmium (CadA) IB pType ATPases also use a
537 carboxylate ligand for zinc and cadmium, respectively, with the presence of a DCxxC motif
538 found in the *E. coli* ZntA and of a Glu residue in a loop more distant of the CxxC motif in the
539 CadA N-terminal domain (Banci et al. 2002; Banci et al. 2006).

540 In conclusion, our analyses highlight the importance of zinc binding to the N-terminal MBD
541 of HMA4 for the protein function *in planta*. This work further establishes the value of
542 combining *in planta* and *in vitro* studies to reveal the structure/function relationships for
543 transmembrane metal transporters. Future developments may possibly include analysing the
544 interaction of the N-terminal domain and its MBD variants with other cytoplasmic domains
545 of HMA4.

546

References

- Abdel-Ghany SE, Müller-Moulé P, Niyogi KK, Pilon M, Shikanai T (2005) Two P-type ATPases are required for copper delivery in *Arabidopsis thaliana* chloroplasts. *Plant Cell* 17:1233-1251 doi:tpc.104.030452 [pii] 10.1105/tpc.104.030452
- Andrés-Colás N et al. (2006) The *Arabidopsis* heavy metal P-type ATPase HMA5 interacts with metallochaperones and functions in copper detoxification of roots. *Plant J* 45:225-236
- Argüello JM (2003) Identification of ion-selectivity determinants in heavy-metal transport P1B-type ATPases. *J Membr Biol* 195:93-108
- Argüello JM, Eren E, González-Guerrero M (2007) The structure and function of heavy metal transport P1B-ATPases. *Biomaterials* 20:233-248 doi:10.1007/s10534-006-9055-6
- Axelsen KB, Palmgren MG (1998) Evolution of Substrate Specificities in the P-Type ATPase Superfamily. *J Mol Evol* 46:84-101 doi:10.1007/pl00006286
- Baekgaard L et al. (2010) A combined zinc/cadmium sensor and zinc/cadmium export regulator in a heavy metal pump. *J Biol Chem* 285:31243-31252 doi:10.1074/jbc.M110.111260
- Banci L, Bertini I, Ciofi-Baffoni S, Finney LA, Outten CE, O'Halloran TV (2002) A New Zinc-protein Coordination Site in Intracellular Metal Trafficking: Solution Structure of the Apo and Zn(II) forms of ZntA(46–118). *J Mol Biol* 323:883-897 doi:[http://dx.doi.org/10.1016/S0022-2836\(02\)01007-0](http://dx.doi.org/10.1016/S0022-2836(02)01007-0)
- Banci L et al. (2006) Structural basis for metal binding specificity: the N-terminal cadmium binding domain of the P1-type ATPase CadA. *J Mol Biol* 356:638-650 doi:10.1016/j.jmb.2005.11.055
- Barry AN, Shinde U, Lutsenko S (2010) Structural organization of human Cu-transporting ATPases: learning from building blocks. *J Biol Inorg Chem* 15:47-59 doi:10.1007/s00775-009-0595-4
- Baum D (2013) The Origin of Primary Plastids: A Pas de Deux or a Ménage à Trois? *Plant Cell* 25:4-6 doi:10.1105/tpc.113.109496
- Bernal M, Testillano PS, Alfonso M, del Carmen Risueño M, Picorel R, Yruela I (2007) Identification and subcellular localization of the soybean copper P1B-ATPase GmHMA8 transporter. *J Struct Biol* 158:46-58 doi:S1047-8477(06)00326-1 [pii] 10.1016/j.jsb.2006.10.016
- Boutigny S et al. (2014) HMA1 and PAA1, two chloroplast-envelope PIB-ATPases, play distinct roles in chloroplast copper homeostasis. *J Exp Bot* 65:1529-1540 doi:10.1093/jxb/eru020
- Broadley MR, White PJ, Hammond JP, Zelko I, Lux A (2007) Zinc in plants. *New Phytol* 173:677-702
- Cavanagh J, Fairbrother, W. E., Palmer, A. G., III, and Skelton, N. J. (1996) *Protein NMR Spectroscopy Principles and Practice*. San Diego
- Chan H et al. (2010) The p-type ATPase superfamily. *J Mol Microbiol Biotechnol* 19:5-104 doi:10.1159/000319588
- Charlier JB et al. (2015) Zinc triggers a complex transcriptional and post-transcriptional regulation of the metal homeostasis gene *FRD3* in *Arabidopsis* relatives. *J Exp Bot* 66:3865-3878 doi:10.1093/jxb/erv188
- Clough SJ, Bent AF (1998) Floral dip: a simplified method for *Agrobacterium*-mediated transformation of *Arabidopsis thaliana*. *Plant J* 16:735-743 doi:10.1046/j.1365-313x.1998.00343.x

- Courbot M, Willems G, Motte P, Arvidsson S, Roosens N, Saumitou-Laprade P, Verbruggen N (2007) A major quantitative trait locus for cadmium tolerance in *Arabidopsis halleri* colocalizes with HMA4, a gene encoding a heavy metal ATPase. *Plant Physiol* 144:1052-1065 doi:10.1104/pp.106.095133
- Craciun AR, Meyer C-L, Chen J, Roosens N, De Groot R, Hilson P, Verbruggen N (2012) Variation in *HMA4* gene copy number and expression among *Noccaea caerulescens* populations presenting different levels of Cd tolerance and accumulation. *J Exp Bot* 63:4179-4189 doi:10.1093/jxb/ers104
- Cun P et al. (2014) Modulation of Zn/Cd P(1B2)-ATPase activities in *Arabidopsis* impacts differently on Zn and Cd contents in shoots and seeds. *Metallomics* 6:2109-2116 doi:10.1039/c4mt00182f
- Curtis MD, Grossniklaus U (2003) A gateway cloning vector set for high-throughput functional analysis of genes in planta. *Plant Physiol* 133:462-469
- Czechowski T, Stitt M, Altmann T, Udvardi MK, Scheible WR (2005) Genome-wide identification and testing of superior reference genes for transcript normalization in *Arabidopsis*. *Plant Physiol* 139:5-17
- Drees SL, Beyer DF, Lenders-Lomscher C, Lübben M (2015) Distinct functions of serial metal-binding domains in the *Escherichia coli* P1B-ATPase CopA. *Mol Microbiol* 97:423-438 doi:10.1111/mmi.13038
- Eren E, González-Guerrero M, Kaufman BM, Argüello JM (2007) Novel Zn²⁺ coordination by the regulatory N-terminus metal binding domain of *Arabidopsis thaliana* Zn(2+)-ATPase HMA2. *Biochemistry* 46:7754-7764 doi:10.1021/bi7001345
- Gaither LA, Eide DJ (2001) Eukaryotic zinc transporters and their regulation. *Biometals* 14:251-270
- Goyer RA (1997) Toxic and essential metal interactions. *Annu Rev Nutr* 17:37-50
- Hall JL, Williams LE (2003) Transition metal transporters in plants. *J Exp Bot* 54:2601-2613 doi:10.1093/jxb/erg303
- Hanikenne M, Baurain D (2014) Origin and evolution of metal P-type ATPases in Plantae (Archaeplastida). *Front Plant Sci* 4:544 doi:10.3389/fpls.2013.00544
- Hanikenne M, Krämer U, Demoulin V, Baurain D (2005) A comparative inventory of metal transporters in the green alga *Chlamydomonas reinhardtii* and the red alga *Cyanidioschizon merolae*. *Plant Physiol* 137:428-446 doi:10.1104/pp.104.054189
- Hanikenne M, Kroymann J, Trampczynska A, Bernal M, Motte P, Clemens S, Krämer U (2013) Hard selective sweep and ectopic gene conversion in a gene cluster affording environmental adaptation. *PLoS Genet* 9:1-13
- Hanikenne M, Nouet C (2011) Metal hyperaccumulation and hypertolerance: a model for plant evolutionary genomics. *Curr Opin Plant Biol* 14:252-259
- Hanikenne M et al. (2008) Evolution of metal hyperaccumulation required *cis*-regulatory changes and triplication of *HMA4*. *Nature* 453:391-395 doi:10.1038/nature06877
- Hellemans J, Mortier G, De Paepe A, Speleman F, Vandesompele J (2007) qBase relative quantification framework and software for management and automated analysis of real-time quantitative PCR data. *Genome Biol* 8:R19
- Hussain D et al. (2004) P-type ATPase heavy metal transporters with roles in essential zinc homeostasis in *Arabidopsis*. *Plant Cell* 16:1327-1339 doi:10.1105/tpc.020487
- Kim YY, Choi H, Segami S, Cho HT, Martinoia E, Maeshima M, Lee Y (2009) AtHMA1 contributes to the detoxification of excess Zn(II) in *Arabidopsis*. *Plant J* 58:737-753 doi:TPJ3818 [pii]10.1111/j.1365-313X.2009.03818.x
- Kobayashi Y et al. (2008) Amino Acid Polymorphisms in Strictly Conserved Domains of a P-Type ATPase HMA5 Are Involved in the Mechanism of Copper Tolerance Variation in *Arabidopsis*. *Plant Physiol* 148:969-980

- Krämer U (2010) Metal hyperaccumulation in plants. *Annu Rev Plant Biol* 61:517-534 doi:10.1146/annurev-arplant-042809-112156
- Krämer U, Talke IN, Hanikenne M (2007) Transition metal transport. *FEBS Lett* 581:2263-2272 doi:10.1016/j.febslet.2007.04.010
- Kühlbrandt W (2004) Biology, structure and mechanism of P-type ATPases. *Nat Rev Mol Cell Biol* 5:282-295 doi:10.1038/nrm1354
- Lian L-Y et al. (2000) Mapping the binding site for the GTP-binding protein Rac-1 on its inhibitor RhoGDI-1. *Structure* 8:47-56 doi:[http://dx.doi.org/10.1016/S0969-2126\(00\)00080-0](http://dx.doi.org/10.1016/S0969-2126(00)00080-0)
- Lutsenko S, Petris MJ (2003) Function and regulation of the mammalian copper-transporting ATPases: insights from biochemical and cell biological approaches. *J Membr Biol* 191:1-12
- Mana-Capelli S, Mandal AK, Argüello JM (2003) *Archaeoglobus fulgidus* CopB is a thermophilic Cu²⁺-ATPase: functional role of its histidine-rich-N-terminal metal binding domain. *J Biol Chem* 278:40534-40541 doi:10.1074/jbc.M306907200
- Mandal AK, Mikhailova L, Argüello JM (2003) The Na,K-ATPase S5-H5 helix: structural link between phosphorylation and cation-binding sites. *Ann N Y Acad Sci* 986:224-225
- Mills RF, Krijger GC, Baccarini PJ, Hall JL, Williams LE (2003) Functional expression of AtHMA4, a P1B-type ATPase of the Zn/Co/Cd/Pb subclass. *Plant J* 35:164-176
- Mills RF, Valdes B, Duke M, Peaston KA, Lahner B, Salt DE, Williams LE (2010) Functional significance of AtHMA4 C-terminal domain in planta. *PLoS One* 5:e13388 doi:10.1371/journal.pone.0013388
- Moreno I et al. (2008) AtHMA1 is a thapsigargin sensitive Ca²⁺/heavy metal pump. *J Biol Chem* 283:9633-9641
- Nouet C, Charlier JB, Carnol M, Bosman B, Farnir F, Motte P, Hanikenne M (2015) Functional analysis of the three *HMA4* copies of the metal hyperaccumulator *Arabidopsis halleri*. *J Exp Bot* 66:5783-5795 doi:10.1093/jxb/erv280
- Nouet C, Motte P, Hanikenne M (2011) Chloroplastic and mitochondrial metal homeostasis. *Trends Plant Sci* 16:395-404 doi:S1360-1385(11)00053-7 [pii] 10.1016/j.tplants.2011.03.005
- O' Lochlainn S et al. (2011) Tandem Quadruplication of *HMA4* in the Zinc (Zn) and Cadmium (Cd) Hyperaccumulator *Noccaea caerulescens*. *PLoS One* 6:e17814
- Palmer CM, Guerinot ML (2009) Facing the challenges of Cu, Fe and Zn homeostasis in plants. *Nat Chem Biol* 5:333-340
- Palmgren MG, Nissen P (2011) P-type ATPases. *Annu Rev Biophys* 40:243-266 doi:10.1146/annurev.biophys.093008.131331
- Pedersen CNS, Axelsen KB, Harper JF, Palmgren MG (2012) Evolution of plant P-type ATPases. *Front Plant Sci* 3:31 doi:10.3389/fpls.2012.00031
- Rausin G, Tillemans V, Stankovic N, Hanikenne M, Motte P (2010) Dynamic nucleocytoplasmic shuttling of an Arabidopsis SR splicing factor: role of the RNA-binding domains. *Plant Physiol* 153:273-284 doi:pp.110.154740 [pii] 10.1104/pp.110.154740
- Seigneurin-Berny D et al. (2006) HMA1, a new Cu-ATPase of the chloroplast envelope, is essential for growth under adverse light conditions. *J Biol Chem* 281:2882-2892 doi:M508333200 [pii] 10.1074/jbc.M508333200
- Shen Y, Delaglio F, Cornilescu G, Bax A (2009) TALOS+: a hybrid method for predicting protein backbone torsion angles from NMR chemical shifts. *J Biomol NMR* 44:213-223 doi:10.1007/s10858-009-9333-z

- Shikanai T, Müller-Moulé P, Munekage Y, Niyogi KK, Pilon M (2003) PAA1, a P-type ATPase of Arabidopsis, functions in copper transport in chloroplasts. *Plant Cell* 15:1333-1346
- Siemianowski O, Barabasz A, Weremczuk A, Ruszczyńska A, Bulska EWA, Williams LE, Antosiewicz DM (2013) Development of Zn-related necrosis in tobacco is enhanced by expressing AtHMA4 and depends on the apoplastic Zn levels. *Plant Cell Environ* 36:1093-1104 doi:10.1111/pce.12041
- Talke IN, Hanikenne M, Krämer U (2006) Zinc-dependent global transcriptional control, transcriptional deregulation, and higher gene copy number for genes in metal homeostasis of the hyperaccumulator *Arabidopsis halleri*. *Plant Physiol* 142:148-167 doi:pp.105.076232 [pii] 10.1104/pp.105.076232
- Tavel L et al. (2012) Ligand Binding Study of Human PEBP1/RKIP: Interaction with Nucleotides and Raf-1 Peptides Evidenced by NMR and Mass Spectrometry. *PLoS ONE* 7:e36187 doi:10.1371/journal.pone.0036187
- Tocquin P, Corbesier L, Havelange A, Pieltain A, Kurtem E, Bernier G, Périlleux C (2003) A novel high efficiency, low maintenance, hydroponic system for synchronous growth and flowering of *Arabidopsis thaliana*. *BMC Plant Biol* 3:2
- Toyoshima C (2008) Structural aspects of ion pumping by Ca²⁺-ATPase of sarcoplasmic reticulum. *Arch Biochem Biophys* 476:3-11 doi:S0003-9861(08)00193-8 [pii] 10.1016/j.abb.2008.04.017
- Toyoshima C (2009) How Ca²⁺-ATPase pumps ions across the sarcoplasmic reticulum membrane. *Biochim Biophys Acta* 1793:941-946 doi:S0167-4889(08)00355-8 [pii] 10.1016/j.bbamcr.2008.10.008
- Toyoshima C, Inesi G (2004) Structural basis of ion pumping by Ca²⁺-ATPase of the sarcoplasmic reticulum. *Annu Rev Biochem* 73:269-292 doi:10.1146/annurev.biochem.73.011303.073700
- Toyoshima C, Nomura H (2002) Structural changes in the calcium pump accompanying the dissociation of calcium. *Nature* 418:605-611 doi:10.1038/nature00944 nature00944 [pii]
- Tsivkovskii R, MacArthur BC, Lutsenko S (2001) The Lys1010-Lys1325 fragment of the Wilson's disease protein binds nucleotides and interacts with the N-terminal domain of this protein in a copper-dependent manner. *J Biol Chem* 276:2234-2242 doi:10.1074/jbc.M003238200
- Tuerk MJ, Fazel N (2009) Zinc deficiency. *Curr Opin Gastroenterol* 25:136-143 doi:10.1097/MOG.0b013e328321b395 00001574-200903000-00009 [pii]
- Vandesompele J, De Preter K, Pattyn F, Poppe B, Van Roy N, De Paepe A, Speleman F (2002) Accurate normalization of real-time quantitative RT-PCR data by geometric averaging of multiple internal control genes. *Genome Biol* 3:RESEARCH0034
- Veldhuis N, Gaeth A, Pearson R, Gabriel K, Camakaris J (2009) The multi-layered regulation of copper translocating P-type ATPases. *BioMetals* 22:177-190 doi:10.1007/s10534-008-9183-2
- Verret F et al. (2004) Overexpression of AtHMA4 enhances root-to-shoot translocation of zinc and cadmium and plant metal tolerance. *FEBS Lett* 576:306-312
- Verret F, Gravot A, Auroy P, Preveral S, Forestier C, Vavasseur A, Richaud P (2005) Heavy metal transport by AtHMA4 involves the N-terminal degenerated metal binding domain and the C-terminal His11 stretch. *FEBS Lett* 579:1515-1522
- Wang K et al. (2014) Structure and mechanism of Zn²⁺-transporting P-type ATPases. *Nature* 514:518-522 doi:10.1038/nature13618
- Willems G, Drager DB, Courbot M, Gode C, Verbruggen N, Saumitou-Laprade P (2007) The genetic basis of zinc tolerance in the metallophyte *Arabidopsis halleri* ssp. *halleri*

- (Brassicaceae): an analysis of quantitative trait loci. *Genetics* 176:659-674
doi:10.1534/genetics.106.064485
- Williams LE, Mills RF (2005) P(1B)-ATPases--an ancient family of transition metal pumps with diverse functions in plants. *Trends Plant Sci* 10:491-502
doi:10.1016/j.tplants.2005.08.008
- Williamson RA, Carr MD, Frenkiel TA, Feeney J, Freedman RB (1997) Mapping the Binding Site for Matrix Metalloproteinase on the N-Terminal Domain of the Tissue Inhibitor of Metalloproteinases-2 by NMR Chemical Shift Perturbation. *Biochemistry* 36:13882-13889 doi:10.1021/bi9712091
- Wong CK, Cobbett CS (2009) HMA P-type ATPases are the major mechanism for root-to-shoot Cd translocation in *Arabidopsis thaliana*. *New Phytol* 181:71-78
doi:10.1111/j.1469-8137.2008.02638.x
- Wong CK, Jarvis RS, Sherson SM, Cobbett CS (2009) Functional analysis of the heavy metal binding domains of the Zn/Cd-transporting ATPase, HMA2, in *Arabidopsis thaliana*. *New Phytol* 181:79-88 doi:10.1111/j.1469-8137.2008.02637.x
- Xiao Z, Gottschlich L, van der Meulen R, Udagedara SR, Wedd AG (2013) Evaluation of quantitative probes for weaker Cu(I) binding sites completes a set of four capable of detecting Cu(I) affinities from nanomolar to attomolar. *Metallomics* 5:501-513
doi:10.1039/c3mt00032j
- Zimmermann M et al. (2009) Metal binding affinities of *Arabidopsis* zinc and copper transporters: selectivities match the relative, but not the absolute, affinities of their amino-terminal domains. *Biochemistry* 48:11640-11654 doi:10.1021/bi901573b

Table 1. Stoichiometry of zinc binding to AhHMA4 C²⁷CTSE³¹ N-terminal variants.

	Ratio protein/Zn
AhHMA4n	0.86
AhHMA4n C ²⁷ A	0.06
AhHMA4n C ²⁸ A	<0.01
AhHMA4n E ³¹ A	0.37
AhHMA4n C ²⁷ A/C ²⁸ A/E ³¹ A	<0.01

Table 2. Affinity of zinc binding to AhHMA4 C²⁷CTSE³¹ N-terminal variants.

Protein	log K_D^a ([Par] _{tot} , 50 μ M)	log K_D^a ([Par] _{tot} , 100 μ M)	average log K_D	log (K_D/K_D (wt))
AtHMA4n ^b	< - 9.40 ^a	- 9.63	- 9.63	~ 0
AhHMA4n	< - 9.47 ^a	- 9.60	- 9.60	0
AhHMA4n C ²⁷ A	- 7.82	- 7.83	- 7.83	1.8
AhHMA4n E ³¹ A	-8.21	- 8.19	- 8.20	1.4
AhHMA4n SS	N.D. ^c			

^a The affinity for zinc was determined at two Par concentrations (50 and 100 μ M) (see Zimmermann et al. 2009).

^b Used as control (described in Zimmermann et al. 2009).

^c Not Detectable.

Figure legends

Fig. 1. Complementation of the *hma2hma4* *A. thaliana* mutant by the *A. halleri* HMA4 protein and C²⁷CTSE³¹ variants expressed under the control of the *pAtHMA4* promoter. **a** Partial sequences of the AhHMA4 N-terminal (AhHMA4n) domain. Mutated residues in the C²⁷CTSE³¹ motif are shown in bold font. **b-j** Phenotype of the plants after 8 weeks of growth on standard soil. Plants were grown without Zn supplementation for phenotyping. Wild-type *A. thaliana* plants (Col-0 accession) (**b**) and the *hma2hma4* mutant (**c-d**) are shown as controls. Mutant plants expressing a native AhHMA4 protein (**e**) or C²⁷A (**g-h**), C²⁸A (**i**), E³¹A (**f**) and triple C²⁷A/C²⁸A/E³¹A (**j**) variants display wild-type (**e**) or mutant phenotypes (**g-j**). Scalebars: 1 cm.

Fig. 2. Zinc and cadmium accumulation in plants expressing AhHMA4n variants. Wild-type *A. thaliana* plants (Col-0 accession), *hma2hma4* mutant and mutant plants expressing a native AhHMA4 protein or C²⁷A, C²⁸A, E³¹A and triple C²⁷A/C²⁸A/E³¹A variants were grown for 4 weeks in Hoagland hydroponic medium containing 0.2 µM ZnSO₄ (**a-b**) or 0.05 µM CdSO₄ (**c-d**). Metal contents (mg kg⁻¹ DW) were measured by ICP-AES from root and shoot tissues. Values relative to the wild-type (Col-0) are means ± SEM of 2-3 independent lines from two independent experiments, each including two replicates of 3 plants per line. The data were analyzed with a Kruskal-Wallis non-parametric ANOVA followed by multiple comparison tests. Statistically significant differences ($p < 0.01$) between means are indicated by different superscripted letters.

Fig. 3. Cellular localization of C²⁷CTSE³¹ AhHMA4 variants. GFP fusions of C²⁷A (**b**), C²⁸A (**c**), E³¹A (**d**) and triple C²⁷A/C²⁸A/E³¹A (**e**) variants were imaged by confocal microscopy in leaves of 18 day-old seedlings. The fusions were expressed in the Col-0 background under the control of a double 35S promoter. Non transformed Col-0 seedlings served as controls (**a**). (**f**) Plasmolysis on leaf of AhHMA4 C²⁸A expressing plants confirmed plasma membrane localization. The arrow indicates a plasmodesmata. Scalebars: 20 µM.

Fig. 4. Superposition of the 2D HSQC ^1H - ^{15}N NMR spectra of the native (in black) and triple $\text{C}^{27}\text{A}/\text{C}^{28}\text{A}/\text{E}^{31}\text{A}$ mutant (in red) AhHMA4n proteins at pH 6.6. The marked peaks (arrows) represent the most affected residues.

Fig. 5. Chemical shift perturbation resulting from the $\text{C}^{27}\text{A}/\text{C}^{28}\text{A}/\text{E}^{31}\text{A}$ mutation in the AhHMA4n protein. **a** A threshold of 3 standard deviations (green line) was selected to identify significant shift perturbations when comparing the native and triple $\text{C}^{27}\text{A}/\text{C}^{28}\text{A}/\text{E}^{31}\text{A}$ mutant AhHMA4n proteins. The green and orange boxes represent the alpha helices and beta sheets in the sequence, respectively. **b** The shift perturbations were localized on the structure of AtHMA4n (2KKH (Zimmermann et al. 2009)) using Pymol. A color code for residues was used to represent the level of perturbation: red $\geq 2\text{ppm}$; $2\text{ppm} \leq \text{purple} \leq 1\text{ppm}$; blue $\leq 1\text{ppm}$.

Figure 1

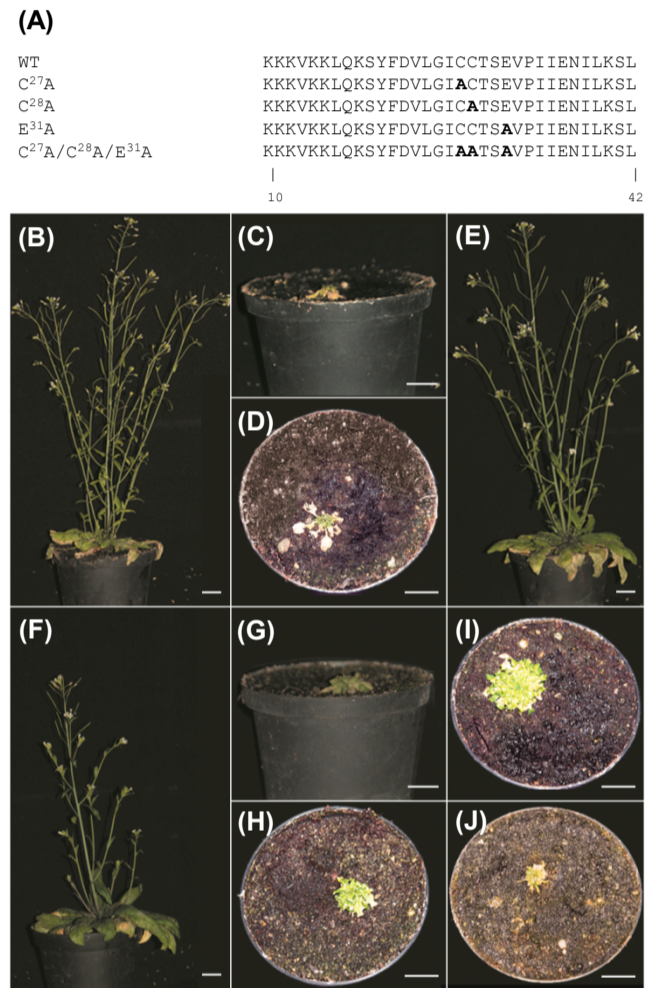


Figure 2

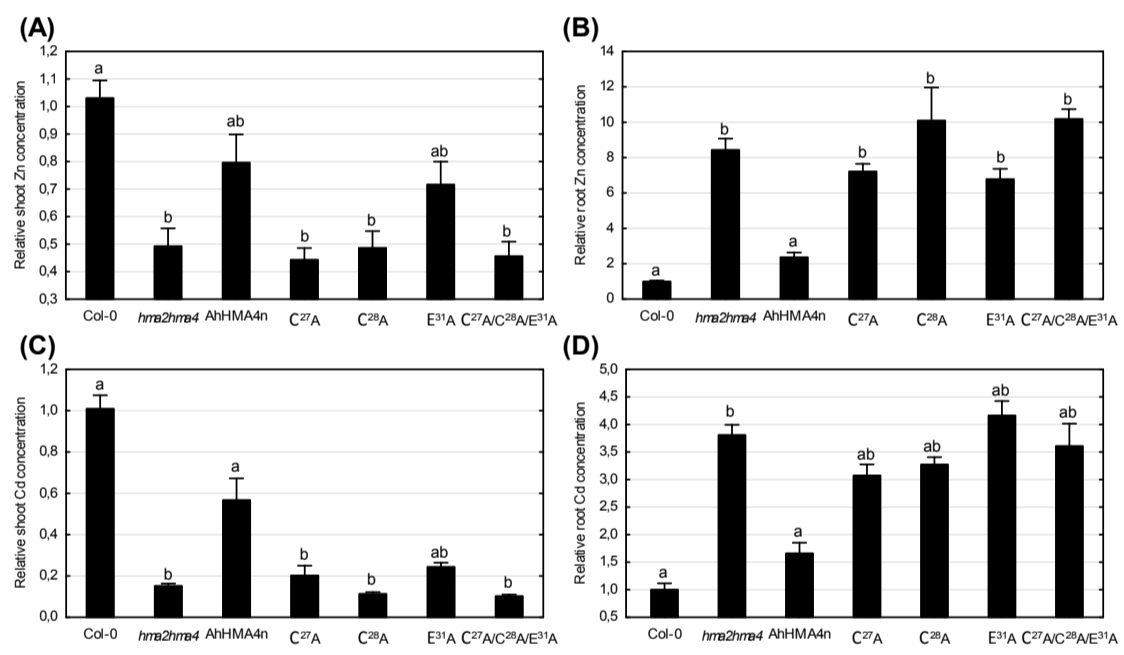


Figure 3

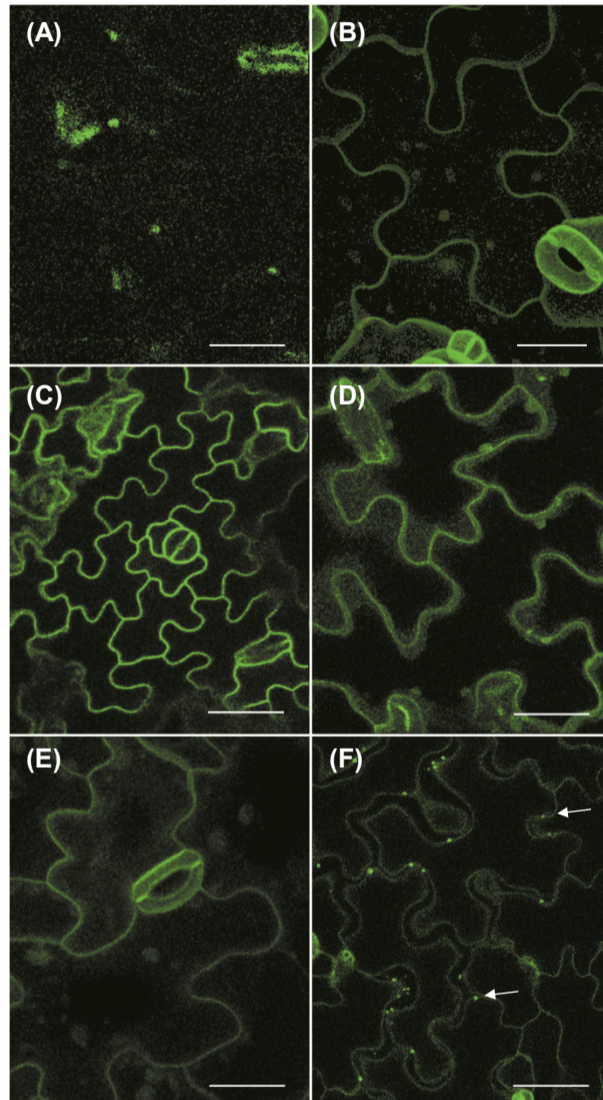


Figure 4

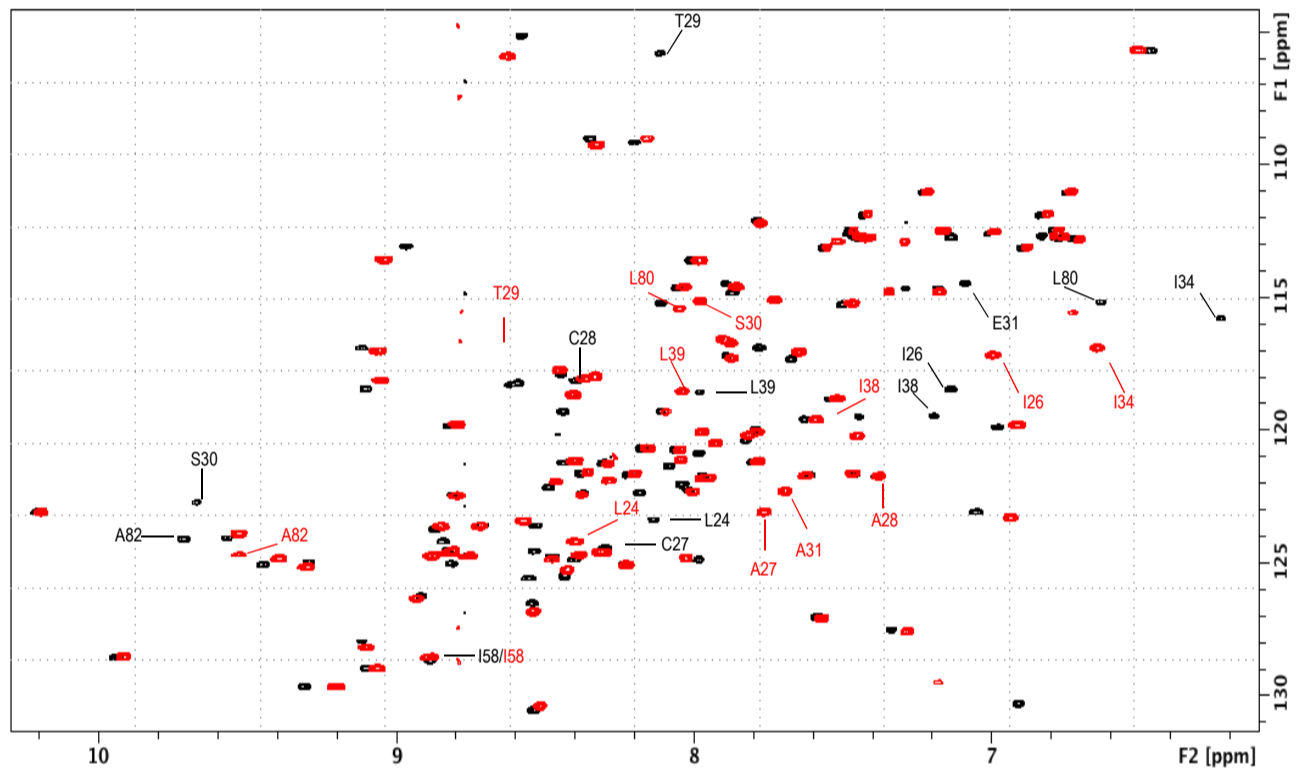
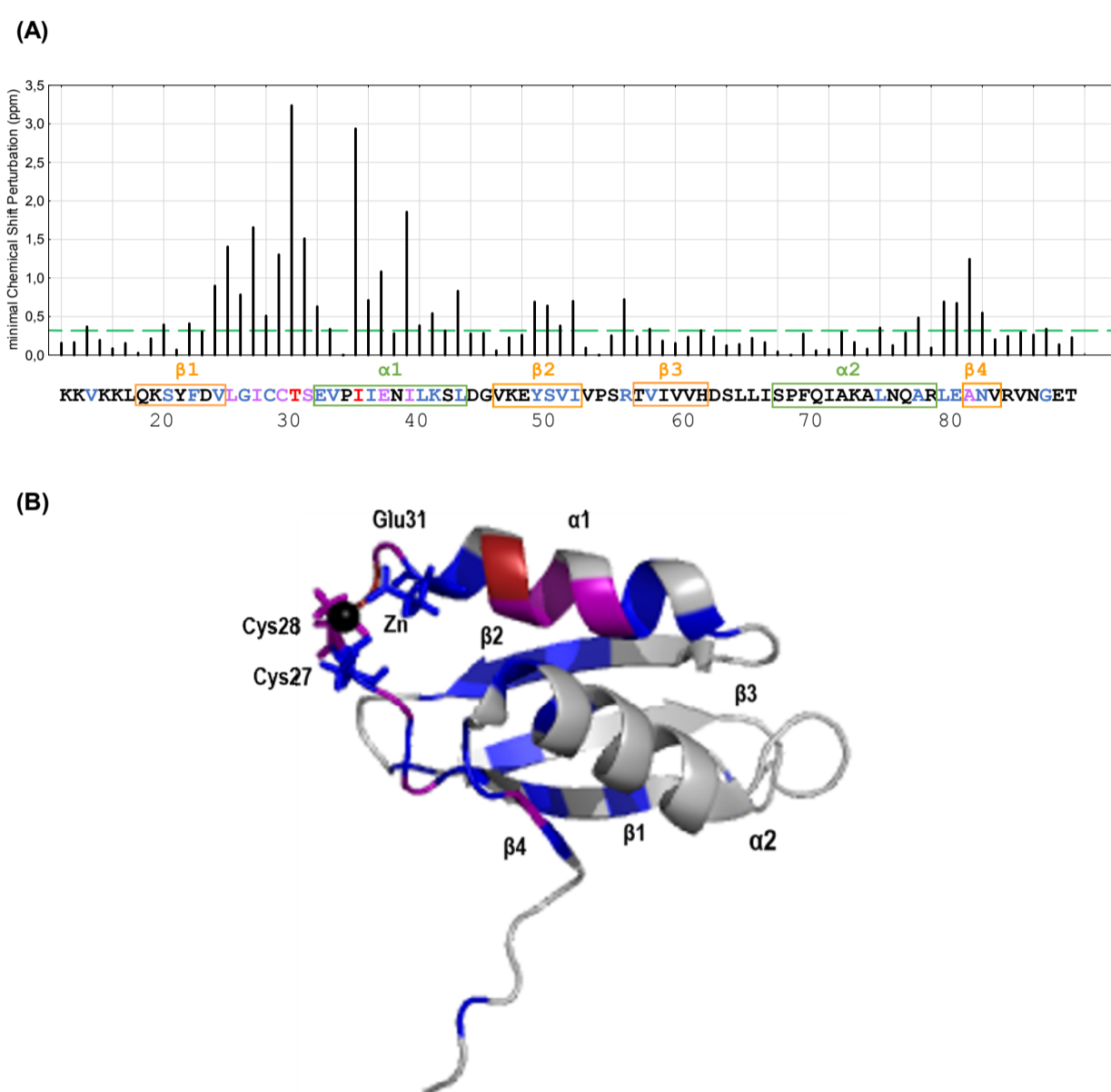


Figure 5



Electronic Supplementary Material

Metal binding to the N-terminal cytoplasmic domain of the P_{1B} ATPase HMA4 is required for metal transport in *Arabidopsis*.

Plant Molecular Biology

Clémentine Laurent¹, Gilles Lekeux¹, Ashwinie A. Ukuwela², Zhiguang Xiao², Jean-Benoit Charlier¹, Bernard Bosman³, Monique Carnol³, Patrick Motte^{1,4}, Christian Damblon⁵, Moreno Galleni¹ and Marc Hanikenne^{1,4,\$}

¹ Center for Protein Engineering (CIP), Department of Life Sciences, University of Liège, B-4000 Liège, Belgium

² School of Chemistry and Bio21 Molecular Science and Biotechnology Institute, University of Melbourne, Parkville, Victoria 3010, Australia

³ Laboratory of Plant and Microbial Ecology, Department of Biology, Ecology, Evolution, University of Liège, B-4000 Liège, Belgium

⁴ PhytoSYSTEMS, University of Liège, B-4000 Liège, Belgium

⁵ Chimie Biologique Structurale, Department of Chemistry, University of Liège, Belgium

^{\$} Corresponding author:

Marc Hanikenne

email: marc.hanikenne@ulg.ac.be

Tel: +32-4-3663844

Fax: +32-4-3662960

Table S1. Primers used in the study.

(A) Cloning primers.

Name	Sequence (5'=>3')
pAthHMA4 AcyI	TTTCTCTTCTTCTTTGTTTTGT GACGCC
pAthHMA4 AscI	TATAGAATTC GGCGCGCC ACTTACCGATCGGGTATGCCATG
AhHMA4 AscI	GGCGCGCC AAGCACTCACATGGTGATGGTGG
AhHMA4 PacI	CC TTAATTAA GGGATGGCGTCACAAAACAAAGAAGAAG

Restriction enzyme sites are indicated in bold font.

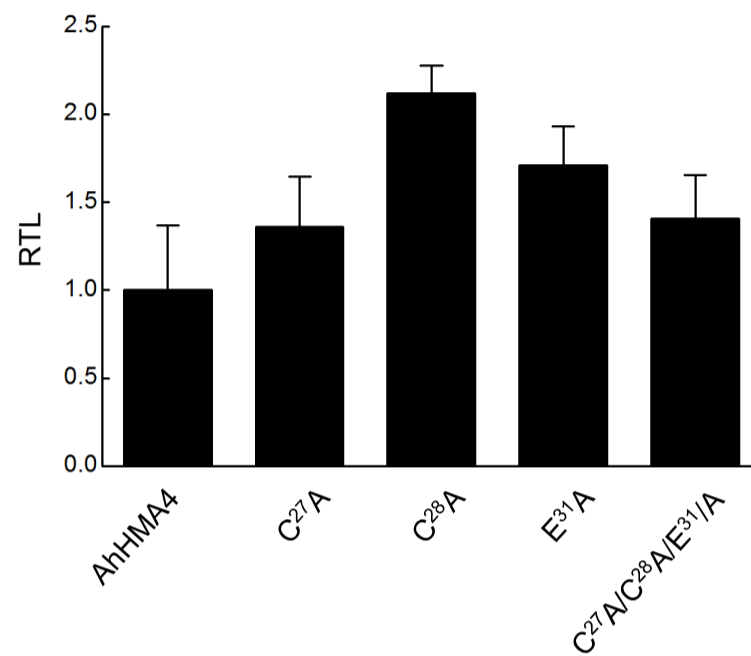
(B) Mutagenic primers.

Name	Sequence (5'=>3')
Full length protein (<i>in vivo</i> experiments)	
AhHMA4 Nter C27A Fwd	GTTACTTCGATGTTCTCGGAAT CGCT TG CAC ATCGGAAGTTCC
AhHMA4 Nter C27A Rev	GGAACTTCCGATGT GCAAGCG ATTCCGAGAACATCGAAGTAAC
AhHMA4 Nter C28A Fwd	CTTCGATGTTCTCGGAATCTGT GC TACATCGGAAGTTCC
AhHMA4 Nter C28A Rev	GGAACTTCCGATGT GC CACAGATTCCGAGAACATCGAAG
AhHMA4 Nter E31A Fwd	CGGAATCTGTT GC CACATCGGC AGT TCTATCATCG
AhHMA4 Nter E31A Rev	CGATGATAGGA ACTG CCGATGT GCA ACAGATTCCG
AhHMA4 Nter C27/AC28A/E31A Fwd	GATGTTCTCGGAAT CGCTGC TACATCGGC TG TCTATCATCGAG
AhHMA4 Nter C27A/C28A/E31A Rev	CTCGATGATAGGAAC AG CCGATGT AGCAGCG ATTCCGAGAACATC
N-terminal domain (<i>in vitro</i> experiments)	
AhHMA4 Nter C27A Fwd	CAGAAATGTTTTCGAT GAT CGGA ACT TCGCTGGTACA AGCA ATACCC
AhHMA4 Nter C27A Rev	GGGTATT GCT TGTACCAGCGAAGTTCCGAT CAT CGAAAACATTCTG
AhHMA4 Nter C28A Fwd	CAGAAATGTTTTCGATGATCGGAACCGCGCTGGT ACA ACAAATACCC
AhHMA4 Nter C28A Rev	GGGTATTTGT TGT ACCAGCGCGGTTCCGAT CAT CGAAAACATTCTG
AhHMA4 Nter E31A Fwd	CAGAAATGTTTTCGAT GAT CGGA ACC CGCTGGTACAACAAATACC
AhHMA4 Nter E31A Rev	GGTATTTGTTGTACCAG CG CGGTTCCGAT CAT CGAAAACATTCTG
AhHMA4 Nter C27A/C28A/E31A Fwd	CAGAAATGTTTTCGAT GAT CGGA ACC CGCTGGT GGCAGCA ATACC
AhHMA4 Nter C27A/C28A/E31A Rev	GGTATT GCTGCC ACCAG CG CGGTTCCGAT CAT CGAAAACATTCTG

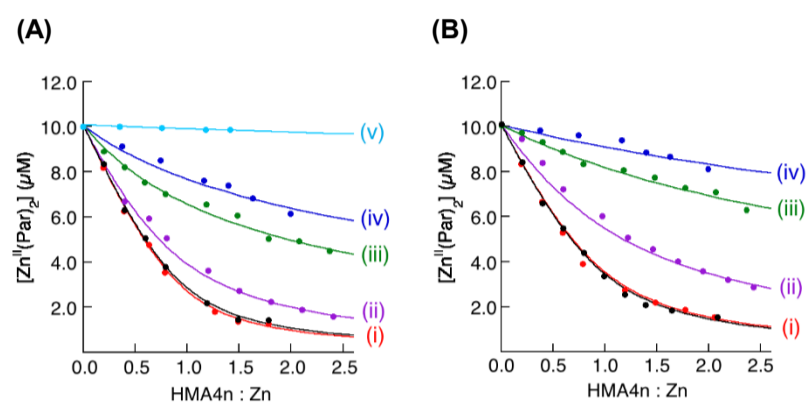
Mutated bases are indicated in bold font.

(C) Real-time RT-PCR primers.

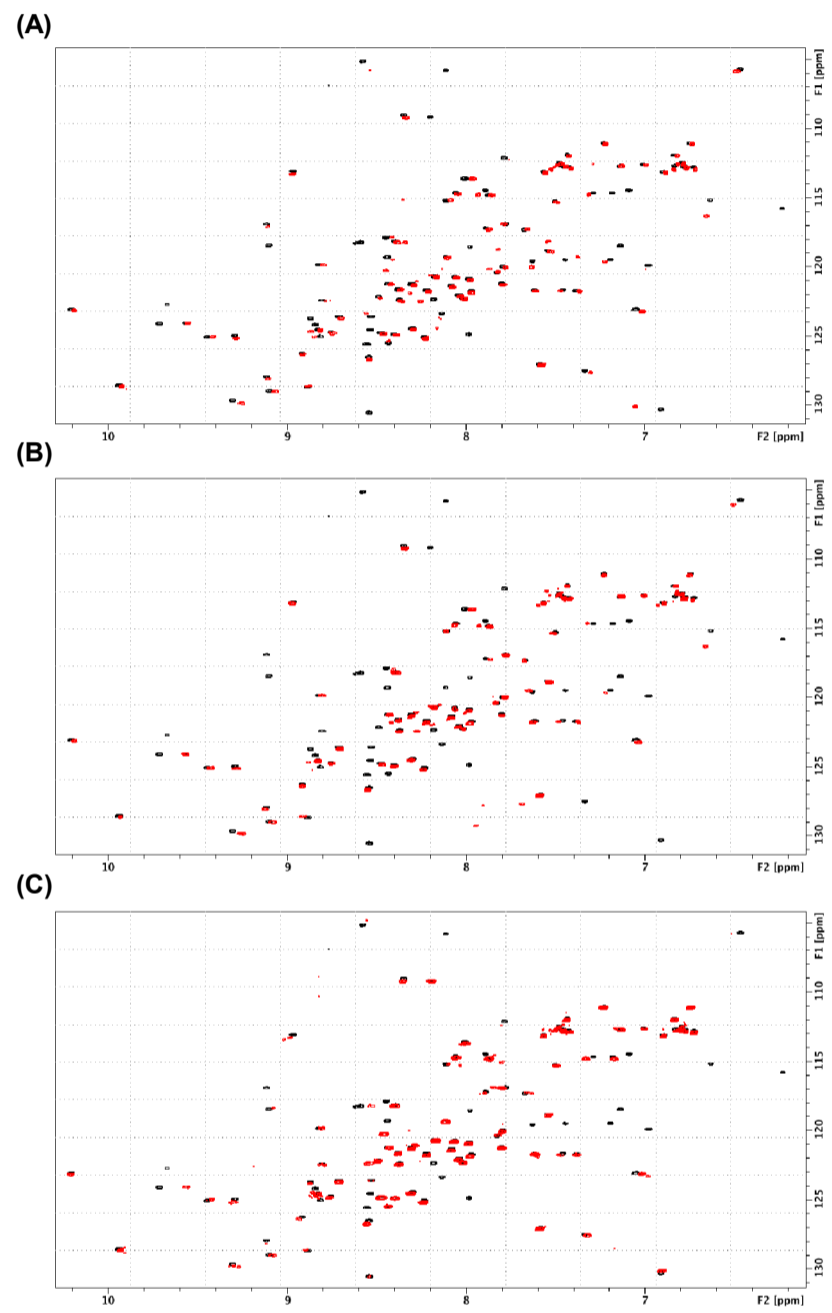
Name	Sequence (5'=>3')
AhHMA4 Fwd	AGCTAGCTACAGGGCGACAGCA
AhHMA4 Rev	CAGCTTTAACCGCTACAACGTGTGCT
EF1a Fwd	TGAGCACGCTCTTCTTGCTTTCA
EF1a Rev	GGTGGTGGCATCCATCTTGTTACA
UBQ10 Fwd	GGCCTTGTATAATCCCTGATGAATAAG
UBQ10 Rev	AAAGAGATAACAGGAACGGAAACATAGT
At1g18050 Fwd	CCATTCTACTTTTGGCGGCT
At1g18050 Rev	TCAATGGTAACTGATCCACTCTGATG



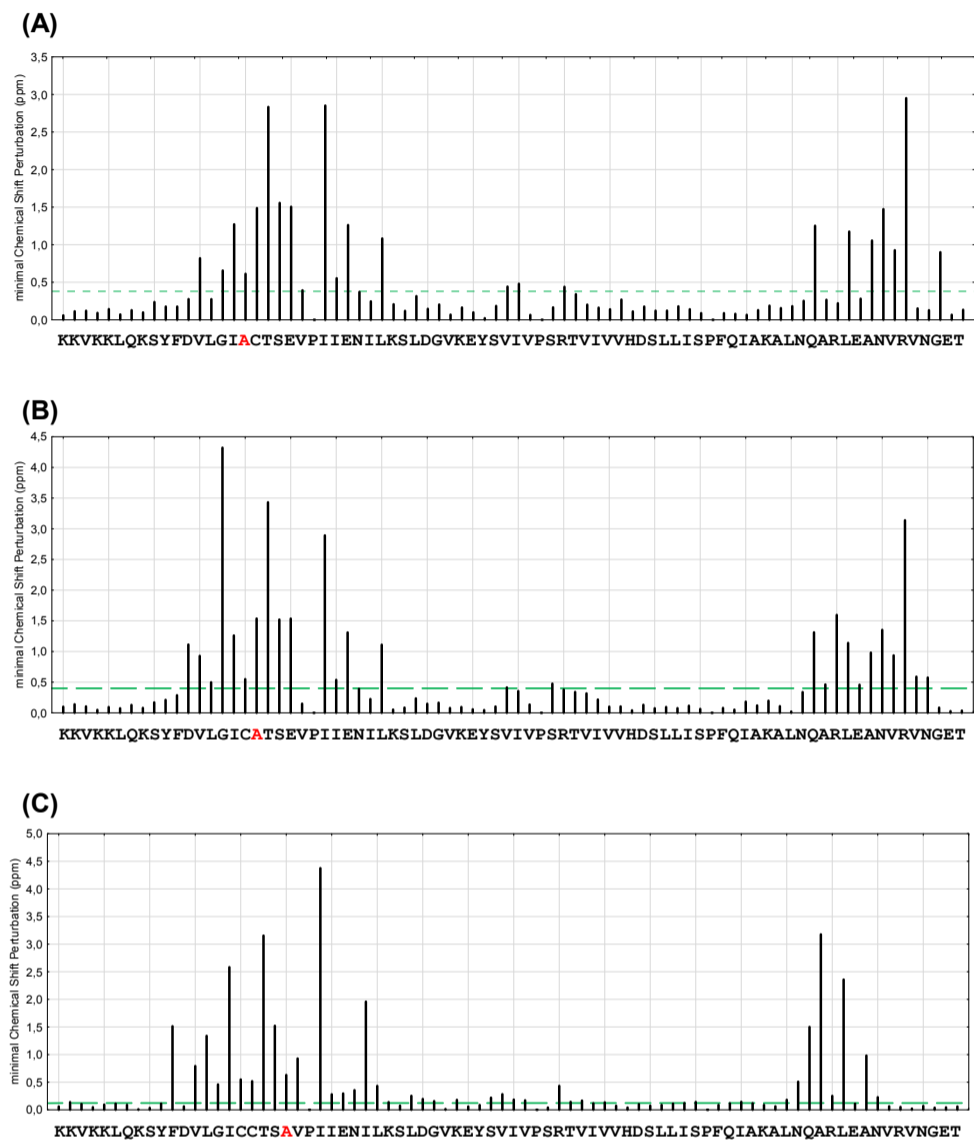
Online Resource 2. Expression of *AhHMA4* in seedlings expressing AhHMA4n variants. *hma2hma4* mutant plants expressing a native AhHMA4 protein or C²⁷A, C²⁸A, E³¹A and triple C²⁷A/C²⁸A/E³¹A variants were grown for 2 weeks on 1/2 MS medium. Expression levels of *AhHMA4* relative to three reference genes (see Methods) and to *AhHMA4* lines are means ± SEM of 2-5 independent lines (>10 seedlings/line). The expression levels are not statistically different (t-test, $p < 0.05$). RTL: Relative Transcript Level.



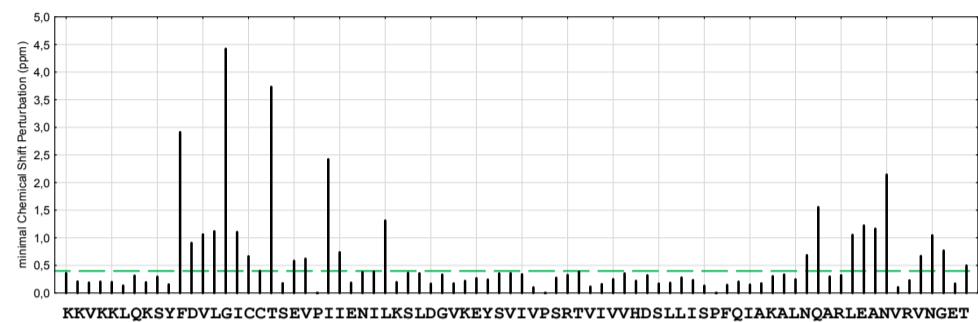
Online Resource 3. Determination of Zn^{II} dissociation constants (K_D) of AhHMA4n native and C²⁷CTSE³¹ variant proteins in MOPS buffer (50 mM, pH 7.3) with the Par ligand as a detection probe and the EGTA ligand as an affinity standard. Variation of $[Zn^{II}(Par)_2]$ with the HMA4n : Zn ratio in the presence of $[Par]_{total} = 50 \mu M$ (a) or $100 \mu M$ (b): (i) native AhHMA4n (in red) and control AtHMA4n (in black, Zimmermann et al. 2009); (ii) control EGTA affinity standard; (iii) E³¹A variant; (iv) C²⁷A variant; (v) oxidized AhHMA4n with an internal disulfide bond. Curve-fittings of the experimental data to eq 2 (see Methods) allowed derivation of $K_D \beta_2 (= (K_{ex})^{-1})$ and the calculation of K_D for Zn^{II} -P via eq 3 (see Methods) with a control reaction involving EGTA and with known K_D for Zn^{II} -EGTA.



Online Resource 4. Superposition of the 2D HSQC ^1H - ^{15}N NMR spectra of the native (in black) and C²⁷A (a), C²⁸A (b) and E³¹A (c) mutant (in red) AhHMA4n proteins at pH 6.6.



Online Resource 5. Chemical shift perturbation at pH 6.6 resulting from the C²⁷A (a), C²⁸A (b) and E³¹A (c) mutations in the AhHMA4n protein. A threshold of 3 standard deviations (green line) was selected to identify significant shift perturbations when comparing the native and mutant AhHMA4n proteins. The mutated residues are in red.



Online Resource 6. Chemical shift perturbation at pH 7.3 resulting from the treatment of the native AhHMA4n protein with EDTA. A threshold of 3 standard deviations (green line) was selected to identify significant shift perturbations when comparing the holo- and apo-forms of the AhHMA4n protein.